J. Earth Syst. Sci. (2021)130 185
https://doi.org/10.1007/s12040-021-01693-0

Protracted Paleozoic–early Triassic thermal events in the Almora nappe, Kumaun Lesser Himalaya, India: Evidence from zircon U–Pb geochronology of Almora paragneiss

Saurabh Gupta and Santosh Kumar*

Department of Geology, Centre of Advanced Study, Kumaun University, Nainital 263 001, India.
**Corresponding author. e-mail: skyadavan@yahoo.com*

MS received 9 April 2021; revised 4 June 2021; accepted 14 June 2021

The Almora nappe in the Kumaun Lesser Himalaya (KLH) is mainly composed of Saryu Formation, Gumalikhet Formation and Cambrian felsic intrusives. Zircons from a paragneiss, exposed near Kwarab along Sualbari–Almora transect, of Saryu Formation, are subjected to U–Pb geochronology in order to delineate the timing of tectono-thermal events and its implication on pre-Himalayan orogenic cycle. Zircon rims developed over Neoarchean–Paleoproterozoic zircon cores record U–Pb ages which broadly correspond to three major pre-Himalayan tectono-thermal (metamorphic) events, early Paleozoic, late Paleozoic and early Triassic. These protracted thermal imprints likely represent the metamorphic episodes experienced by the rocks of Almora nappe. The observed early Triassic rim ages of zircons from paragneiss are very well correlatable with the opening-closure of the Palaeo-Tethys Ocean.

Keywords. Zircon chronology; thermal events; paragneiss; Almora nappe; Kumaun Lesser Himalaya.

1. Introduction

The Himalayan orogeny-related tectono-thermal (metamorphic) events have been recorded on a vast scale during the Tertiary period in response to regional crustal shortening and tectonic burial (Godin 2003). The implication of Himalayan metamorphism on the geodynamic evolution of Himalaya has been described by a number of workers (Gehrels *et al.* 2006 and references therein). Although the pre-Himalayan tectono-magmatic and metamorphic records particularly during the Paleozoic in the Himalaya are widespread (Gehrels *et al.* 2006; Bhargava *et al.* 2016), the still younger pre-Himalayan tectono-thermal (metamorphic) records are yet to be construed because of the fact that the Pre-Himalayan architecture of northern Indian block (NIB) has had very close proximity to the Proto-Tethyan ocean (e.g., Song *et al.* 2020). A number of tectono-magmatic and metamorphic thermal events have equally participated in the episodic crustal growth of East Gondwana. However, no reasonable attempt has been made so far in this regard. In this paper, we report for the first time U–Pb zircon geochronologic data from a paragneiss of Almora nappe, Kumaun Lesser Himalaya, India in order to delineate the timing of pre-Himalayan tectono-thermal (metamorphic) events and its possible implication on understanding the pre-Himalayan orogenic cycles.

Published online: 09 September 2021

2. Geological background

The Main Central Thrust (MCT) bounds the Lesser Himalayan Belt (LHB) in the north and Main Boundary Thrust (MBT) in the south (figure 1a). The LHB marks the presence of numerous thrust sheets (nappes) and klippen. The Almora nappe is one of the largest Himalayan nappes, which lies in the Kumaun Lesser Himalaya extending from Western Nayar to Kali and farther east through Dadeldhura area of western Nepal (Valdiya 1980). Two tectonic units are part of the Almora nappe, viz., the Ramgarh nappe, and the tectonically overlying Almora nappe (e.g., Joshi and Tiwari 2009; Patel *et al.* 2015). The rocks within the Almora nappe, known as Almora Group, are divided into lower Saryu Formation, intrusive granite and granite gneiss, and Gumalikhet Formation (Valdiya 1980). The Saryu Formation is intruded by Cambro–Ordovician granites and granite gneisses in the Champawat and Almora regions (Trivedi *et al.* 1984). The felsic intrusions of similar age also occur in the Dadeldhura nappe in the Nepal, considered as an eastern extension of Almora nappe (Gehrels *et al.* 2006).

A total of four metamorphic zones related to pre-Himalayan regional metamorphism has been recognized from the metapelites of Saryu Formation exposed along the Chhara–Someshwar transect (Joshi and Tiwari 2009) (figure 1b). The pre-Himalayan thermal events are responsible for developing these four metamorphic zones. Based on critical mineral assemblages, the recognized metamorphic zones are chlorite–biotite (zone I), garnet–biotite (zone II), kyanite–biotite (zone III) and sillimanite–K-feldspar (zone IV) (Joshi and Tiwari 2009).

3. Material and methods

A paragneiss sample (AMGn-1) is selected from close to Kwarab area along the Bhowali–Almora road (figure 1b). Zircons were separated from this sample following a conventional method of crushing, magnetic, and heavy liquid separation. Zircons were handpicked under a binocular microscope at National Facility on Low-temperature Thermochronology (Fission Track Dating), Kurukshetra University, Kurukshetra. Approximately 100 zircon grains were mounted on an adhesive tape, enclosed in the epoxy resin, and polished. Zircon morphology was documented under transmitted and reflected light. The internal structures of zircons were examined using cathode-luminescence (CL) image technique at State Key

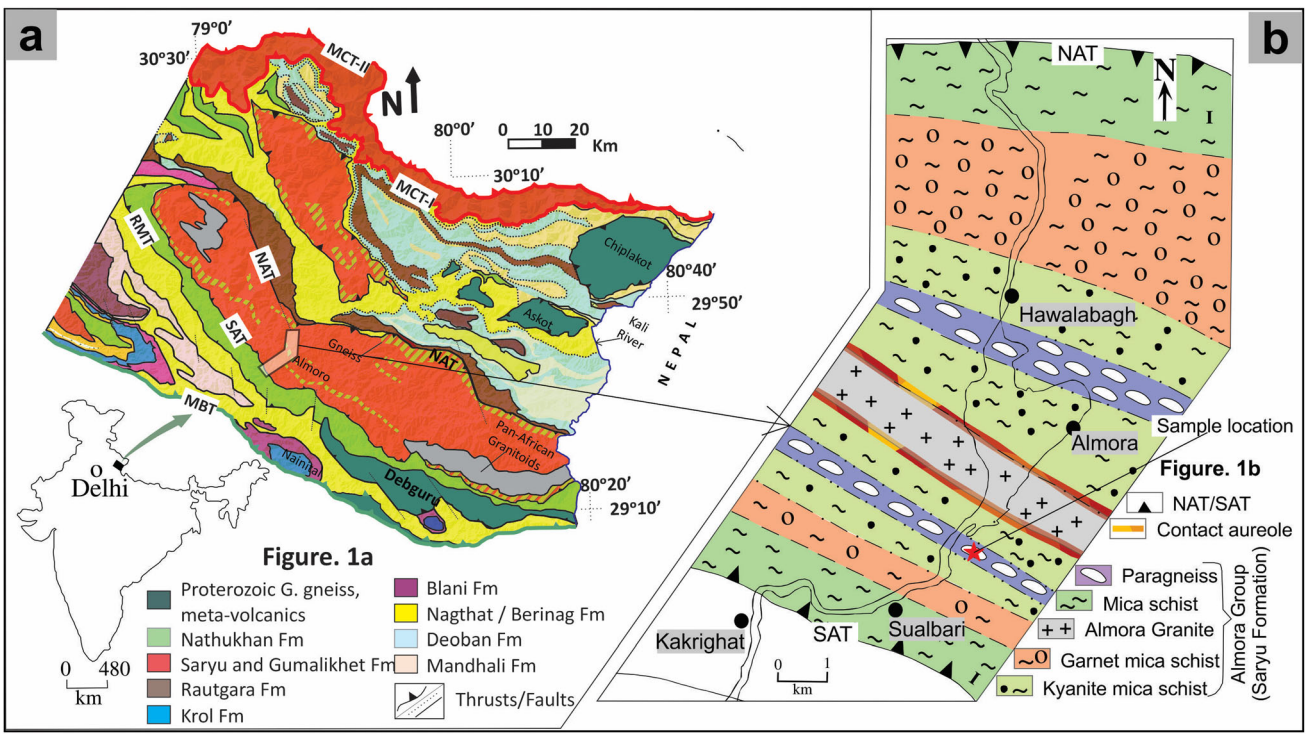

Figure 1. (**a**) Part of the geological map of Kumaun Lesser Himalaya (after Valdiya 1980). (**b**) Lithotectonic units along part of the Chhara–Kakrighat–Hawalabagh–Someshwar transect as shown by Joshi and Tiwari (2009).

Laboratory for Mineral Deposits Research, Nanjing University, China.

The inclusion-free zircon spots were targeted for U–Th–Pb isotope analysis using an Agilent 7500a ICP-MS equipped with a New Wave 213 nm laser, installed at State Key Laboratory of Mineral Deposits Research, Nanjing University, China following the procedure described by Jackson *et al.* (2004). A laser beam diameter of 25 μm, 5 Hz repetition rate, and energy of 10–20 J/cm^2 were used for the isotope measurements. Data acquisition for each analysis took 100 s (40 s on the background and 60 s on signal). The ^{206}Pb, ^{207}Pb, ^{208}Pb, ^{232}Th, and ^{238}U isotopes were analyzed with a dwell time on each isotope of 15, 30, 10, 10, and 15 ms. Zircon GJ-1 was used as an external standard for mass bias and instrument drift correction. Well-characterized Mud Tank (MT) zircon was analyzed to monitor the consistency and solidity of equipment. The weighted mean U–Pb ages, concordia plots, and KDE (Kernel density estimate) were processed using IsoplotR software (Vermeesch 2018).

4. Results

Zircons from a paragneiss (AMGGn-1) are euhedral, elongated, elliptical, and translucent without any radial centre, and vary commonly in size from a few tens of micrometers to several hundred micrometers. Almost all the zircons show prominent bright coloured core and dark coloured rims in CL images. Most zircon cores are euhedral and oscillatory zoned, whereas the rims are usually devoid of zoning (figure 2a–d). The width of the zircon rims varies widely mostly having Th/U < 0.1, while the rims generally have Th/U > 0.1 (table 1). The observed CL images and Th/U ratios of zircons from the paragneiss indicate magmatic cores and metamorphic rims (e.g., Corfu *et al.* 2003).

A total of 30 zircon spots were analyzed from a paragneiss (AMGGn-1) and U–Th–Pb isotopic results are summarized in table 1. Eleven darker rims and nineteen brighter cores were targeted for isotope determination. Out of 19 magmatic zircon cores, four spots produced ^{207}Pb/^{206}Pb concordant Neoarchean to Paleoproterozoic ages ranging from ∼2554 to 1806 Ma (table 1; figure 2b). From the remaining 15 zircon cores, 13 yielded ^{206}Pb/^{238}U concordant Mesoproterozoic to Neoproterozoic ages varying from ∼1126 to 664 Ma (table 1; figure 2d). Unlike older magmatic zircon cores, metamorphic zircon rims are Paleozoic to early Triassic. Out of 11 zircon rims, six zircon rim spots portray concordant age at 490.21 ± 1.29 Ma (MSWD = 0.29). However, from rest of the five zircon rim, four spots produced concordant ^{206}Pb/^{238}U ages varying from ∼423 to 245 Ma (table 1; figure 2c).

5. Discussion and conclusions

This study reports zircon rim (metamorphic) with concordia age at 490.21 ± 1.29 Ma ($n = 6$, MSWD = 0.29), and even still younger concordant late Paleozoic to early Triassic ages (∼423–245 Ma) of zircon rims can also be recorded (figure 2c and table 1) from the studied paragneiss of Almora nappe. However, the zircon magmatic cores have yielded concordant Neoarchean to Paleoproterozoic ages (figure 2b, d; table 1). The record of early Paleozoic metamorphism in the Himachal Lesser Himalaya has already been reported from Naura Formation of the Jutogh Group (Bhargava *et al.* 2016). The present study reports for the first time the record of pre-Himalayan metamorphic events imprinted on the zircon rims of the paragneiss from Almora nappe. Bhargava *et al.* (2016) have dated two garnet crystals using Sm–Nd isotopic method and assigned 479.7 ± 8.5 Ma of metamorphism, which is correlatable well with the observed 490.21 ± 1.29 Ma of zircon metamorphic rims in the paragneiss. Additionally the zircon rims from Almora paragneiss recorded a number of still younger late Paleozoic–early Triassic ages (ca. 423–245 Ma). It is, therefore, proposed that the protracted thermal events (Paleozoic–early Mesozoic) leading to metamorphism operated during the pre-Himalayan orogenic cycle. The observed ∼490 Ma old metamorphic zircon rims represent the most prominent tectono-thermal phase, which coincides well with the global Pan-African–India related thermal events forming a felsic magmatic belt widespread in the Lesser Himalaya of India, Nepal and Bhutan (Gehrels *et al.* 2006; Bhargava *et al.* 2016). About 490 Ma old vast felsic magmatism not only developed contact metamorphic aureoles on the country rocks, rather it was equally responsible for early Paleozoic regional metamorphism in the LHB. Yet the recorded younger metamorphic ages (Paleozoic to early Triassic) of zircon rims may have consequently imposed a regional effect.

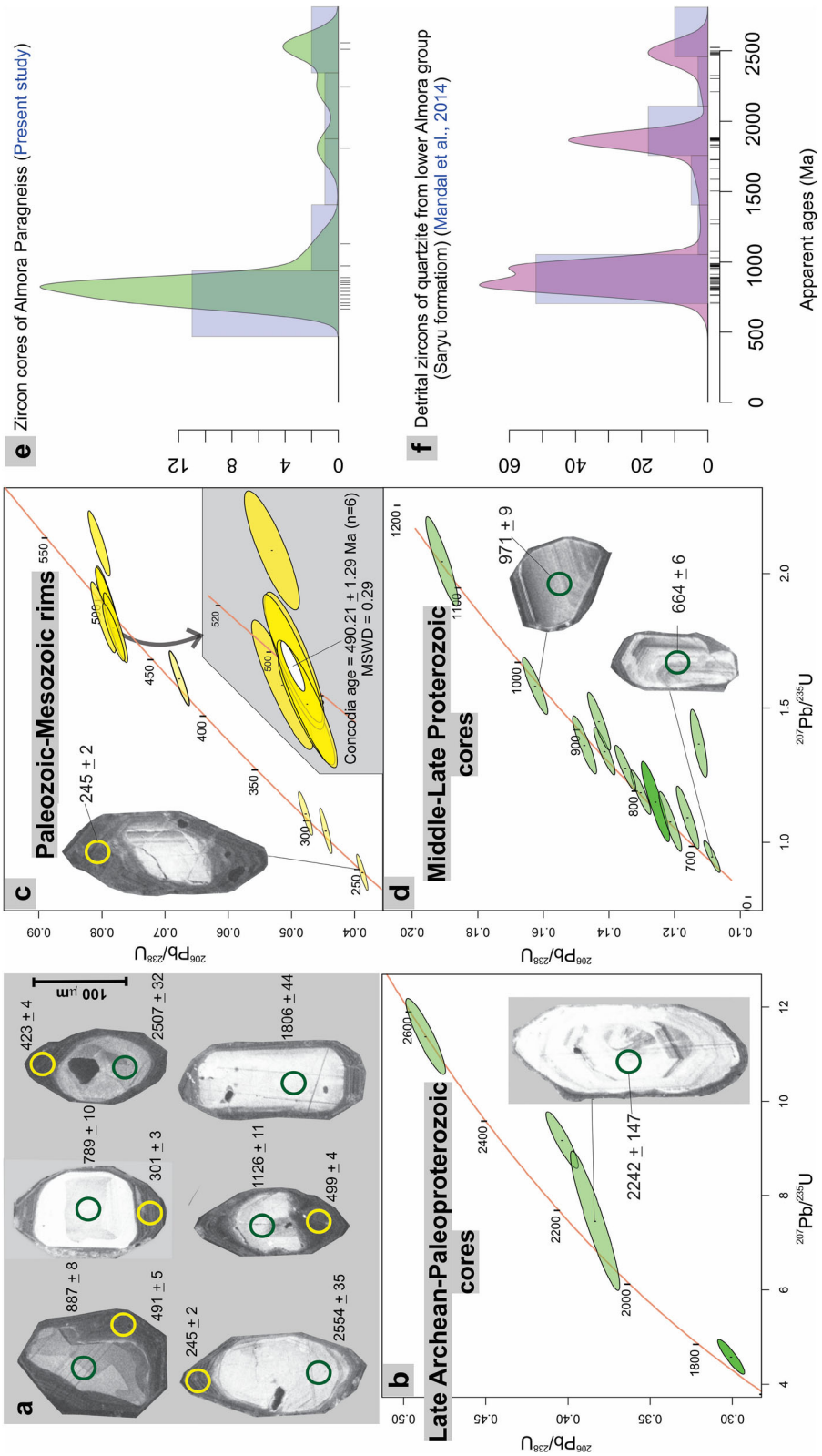

Figure 2. (**a**) Selected CL images of zircons from Almora paragneiss (circles represent the targeted spots for U–Th–Pb isotopes); (**b**, **d**) $^{207}Pb/^{235}U$ *vs.* $^{206}Pb/^{238}U$ Concordia plot of zircon cores of Almora paragneiss; (**c**) $^{207}Pb/^{235}U$ *vs.* $^{206}Pb/^{238}U$ Concordia plot of zircon rims of Almora paragneiss; (**e**) the KDE plot of zircon cores of Almora paragneiss; and (**f**) the KDE plot of detrital zircons of quartzite from lower Saryu Formation (after Mandal *et al.* 2014).

Table 1. *Zircon U–Pb isotopic data of Almora paragneiss (AMGn-1) from Kumaun Lesser Himalaya, India.*

		Common Pb corrected ratios						Error	Ages (Ma)						Discordance
Sample spots	Th/U	$^{207}Pb/^{206}Pb$	1s	$^{207}Pb/^{235}U$	1s	$^{206}Pb/^{238}U$	1s	correlation	$^{207}Pb/^{206}Pb$	1s	$^{207}Pb/^{235}U$	1s	$^{206}Pb/^{238}U$	1s	%
AMGn-1-02_C	0.62	0.06644	0.00365	1.15234	0.0614	0.1258	0.00174	0.9	820	88	778	29	764	10	5.12
AMGn-1-03_C	0.88	0.06607	0.00201	1.18679	0.03377	0.13028	0.00126	0.9	809	43	794	16	789	7	1.85
AMGn-1-05_C	0.45	0.06874	0.00197	1.33942	0.03577	0.14132	0.00133	0.9	891	39	863	16	852	8	3.14
AMGn-1-08_C	0.49	0.06833	0.00312	1.09297	0.04789	0.11601	0.00141	0.9	879	71	750	23	708	8	14.68
AMGn-1-10_C	1.50	0.06705	0.00229	1.36306	0.04382	0.14744	0.00149	0.9	839	50	873	19	887	8	−4.05
AMGn-1-15_C	0.49	0.06443	0.00285	1.07738	0.04563	0.12129	0.00141	0.9	756	70	742	22	738	8	1.85
AMGn-1-16_C	0.37	0.0687	0.00196	1.2779	0.0343	0.13498	0.0013	0.9	890	39	836	15	816	7	6.07
AMGn-1-20_C	0.49	0.06326	0.00174	0.94671	0.02434	0.10858	0.00102	0.9	717	39	676	13	664	6	5.72
AMGn-1-22_C	0.73	0.0706	0.00206	1.58171	0.04333	0.16255	0.00157	0.9	946	40	963	17	971	9	−1.80
AMGn-1-06_C	0.23	0.08815	0.00341	1.36835	0.05142	0.11259	0.00106	0.79	1386	76	875	22	688	6	36.87
AMGn-1-07_C	0.35	0.07357	0.00237	1.45052	0.04391	0.143	0.00143	0.9	1030	45	910	18	862	8	11.65
AMGn-1-09_C	0.06	0.07259	0.00194	0.32162	0.00788	0.03214	0.00029	0.9	1003	35	283	6	204	2	71.78
AMGn-1-11_C	1.17	0.07767	0.00273	2.04432	0.06793	0.1909	0.00201	0.9	1138	49	1130	23	1126	11	0.70
AMGn-1-01_C	0.12	0.07908	0.00244	0.58912	0.01737	0.05403	0.00049	0.82	1174	62	470	11	339	3	59.97
AMGn-1-12_C	0.06	0.14592	0.00409	2.79423	0.07398	0.13888	0.00126	0.88	2299	49	1354	20	838	7	63.55
AMGn-1-13_C	0.75	0.11041	0.00388	4.57846	0.15133	0.30078	0.00332	0.9	1806	44	1745	28	1695	16	6.15
AMGn-1-14_C	0.97	0.16963	0.00528	11.37923	0.32918	0.48655	0.00493	0.9	2554	35	2555	27	2556	21	−0.08
AMGn-1-24_C	1.67	0.16499	0.00472	9.17816	0.24659	0.40359	0.00402	0.9	2507	32	2356	25	2186	18	12.80
AMGn-3-30_C	0.54	0.14123	0.01167	7.4672	0.60538	0.38346	0.00614	0.93	2242	147	2169	73	2092	29	6.69
AMGn-3-17_R	0.42	0.05487	0.00158	0.59118	0.01605	0.07818	0.00074	0.9	407	44	472	10	485	4	−15.97
AMGn-3-19_R	0.03	0.0639	0.00169	0.70889	0.01767	0.08046	0.00072	0.85	738	57	544	10	499	4	26.29
AMGn-3-21_R	0.04	0.0577	0.00196	0.62861	0.02044	0.07901	0.00078	0.85	518	76	495	13	490	5	4.44
AMGn-3-23_R	0.02	0.05677	0.00169	0.53017	0.01486	0.06776	0.00065	0.9	483	45	432	10	423	4	10.56
AMGn-3-25_R	0.13	0.05779	0.00184	0.63033	0.01906	0.07913	0.00078	0.9	522	49	496	12	491	5	4.98
AMGn-3-26_R	0.36	0.05556	0.00184	0.61116	0.01925	0.0798	0.0008	0.9	435	52	484	12	495	5	−11.26
AMGn-3-29_R	0.11	0.05541	0.00184	0.59737	0.01894	0.07821	0.00079	0.9	429	53	476	12	485	5	−10.96
AMGn-3-04_R	0.05	0.05335	0.00208	0.32782	0.01242	0.04456	0.0004	0.76	344	90	288	10	281	2	16.28
AMGn-3-27_R	0.03	0.05098	0.00191	0.27247	0.00989	0.03877	0.00037	0.79	240	89	245	8	245	2	−2.08
AMGn-3-28_R	0.03	0.05327	0.00188	0.35077	0.01192	0.04776	0.00046	0.83	340	82	305	9	301	3	10.29
AMGn-3-18_R	13.47	0.06366	0.00179	0.1947	0.00512	0.02219	0.00021	0.9	730	40	181	4	141	1	75.21

Interestingly, Himalayan orogeny-related thermal record is not imprinted on the zircons of paragneiss, which could be because of development of less prominent zircon rims during the Himalayan orogenesis, and the zircon rims <20 μm cannot be targeted for *in-situ* isotope determination using LA-ICP-MS. It is likely that the *P–T* conditions acted upon the Almora paragneiss during the Himalayan orogeny were not so pertinent to develop prominent metamorphic rims over the zircons of paragneiss. Mandal *et al.* (2014) have dated the detrital zircons from a thin-bedded quartzite horizon of lower Saryu Formation and a thick-bedded quartzite of upper Gumalikhet Formation. They found that the ages of detrital zircons from lower Saryu Formation vary between ∼2526 and 703 Ma, whereas the ages of detrital zircons from Gumalikhet Formation vary between ∼3873 and 538 Ma. A comparative KDE plot of zircon cores from Almora paragneiss (present study) and detrital zircons of lower Saryu Formation (Mandal *et al.* 2014) provide more-or-less similar age spectra and peaks (figure 2e and f). Since both have shown Neoarchean–Paleoproterozoic age spectra, and hence it is more likely that the rocks of lower Saryu Formation might have acted as probable protolith of the Almora paragneiss.

5.1 *Implication for late Paleozoic–early Triassic tectonics of East Gondwana*

The East Gondwana mainly comprises India, Australia, and East Antarctic, and several other small China and Indo-China blocks (e.g., Metcalfe 2013). During the period of successive opening and closure of three intervening Tethyan seas, the Palaeo-Tethys (Devonian–Triassic), Meso-Tethys (late to early Permian–late Cretaceous), and Ceno-Tethys (late Triassic–late Cretaceous), the divergence and northward movement of the numerous continental terranes/blocks from Gondwana took place (Metcalfe 2013). More recently, Song *et al.* (2020) have discovered younger detrital zircons (223–273 Ma) from late Paleozoic to Triassic sedimentary rocks of Gongshan–Baoshan Block in the SE Tibet. They suggested the timing of subduction of the Paleo-Tethys Ocean, which was initiated at ∼273 Ma and closed at ∼223 Ma. Kumar *et al.* (2017) have also found the Permo-Triassic thermal record on the zircon of Cambrian felsic intrusives from the Shillong plateau. The sporadic records of protracted thermal imprints (Paleozoic–Triassic) on the rocks of Lesser Himalayan and adjoining terrains should have been linked with the Neo-Tethys rifting and break-off of Cimmerian terranes around the Artinskian stage which started earlier prior to the closure of Paleo-Tethys (280 Ma–290 Ma) (Angiolini *et al.* 2015).

The observed younger zircon rims (∼245 to 301 Ma) in the present study appear to be swayed from opening and closure of the Palaeo-Tethys Ocean. It is therefore proposed that the Lesser Himalayan rocks were also affected thermally to a certain extent during the opening and closure of Palaeo-Tethys Ocean. However, to make any conclusive remark on the East Gondwana episodic crustal growth and its thermal records, a detailed tectono-metamorphic investigation on the rocks of Lesser Himalayan Belt is required.

Acknowledgements

The present research is supported under a Ministry of Earth Science (MoES) research grant (MoES/P.O.(Geo)/101(v)/2017) awarded to SK. A CSIR-JRF/SRF (09/428(0072)/2013-EMR-1) Fellowship awarded to SG is highly acknowledged. The facility of zircon U–Pb isotope analysis extended by Prof Xisheng-Xu at Nanjing University, China is thankfully acknowledged. Authors thank two anonymous reviewers and Rajneesh Bhutani, the Handling Editor, for providing generous scientific comments that improved the earlier version of the manuscript.

Author statement

Saurabh Gupta: Data curation, format analysis, investigation, methodology, visualization, validation, writing, and editing. Santosh Kumar: Project administration, resources, supervision, data curation, format analysis, investigation, methodology, visualization, validation, writing, review, and editing.

References

Angiolini L, Zanchi A, Zanchetta S, Nicora A, Vuolo I, Berra F, Henderson C, Malaspina N, Rettori R, Vachard D and Vezzoli G 2015 From rift to drift in South Pamir (Tajikistan): Permian evolution of a Cimmerian terrane; *J. Asian Earth Sci.* **102** 146–169, https://doi.org/10.1016/j.jseaes.2014.08.001.

Bhargava O N, Thöni M and Miller C 2016 Isotopic evidence of Early Paleozoic metamorphism in the Lesser Himalaya (Jutogh Group), Himachal Pradesh, India: Its implication; *Him. Geol.* **37**(**2**) 73–84.

Corfu F, Hanchar J M, Hoskin P W O and Kinny P 2003 Atlas of Zircon Textures; *Rev. Mineral. Geochem.* **53**(**1**) 469–500.

Gehrels G E, DeCelles P G, Ojha T P and Upreti B N 2006 Geologic and U–Pb geochronologic evidence for early Paleozoic tectonism in the Dadeldhura thrust sheet, far-west Nepal Himalaya; *J. Asian Earth Sci.* **28** 385–408.

Godin L 2003 Structural evolution of the Tethyan sedimentary sequence in the Annapurna area, central Nepal Himalaya; *J. Asian Earth Sci.* **22** 307–328.

Jackson S E, Pearson N J, Griffin W L and Belousova E A 2004 The application of laser ablation-inductively coupled plasma-mass spectrometry to *in-situ* U–Pb zircon geochronology; *Chem. Geol.* **211** 47–69.

Joshi M and Tiwari A N 2009 Structural events and metamorphic consequences in Almora Nappe, during Himalayan collision tectonics; *J. Asian Earth Sci.* **34** 326–335.

Kumar S, Rino V, Hayasaka Y, Kimura K, Raju S, Terada K and Pathak M 2017 Contribution of Columbia and Gondwana Supercontinent assembly- and growth-related magmatism in the evolution of the Meghalaya Plateau and the Mikir Hills, Northeast India: Constraints from U–Pb SHRIMP zircon geochronology and geochemistry; *Lithos* **277** 356–375.

Mandal S, Robinson D M, Khanal S and Das O 2014 Redefining the tectono-stratigraphic and structural architecture of the Almora klippe and the Ramgarh-Munsiari thrust sheet in NW India; *Geol. Soc. London*; *Spec. Publ.* **412** 247–269.

Metcalfe I 2013 Gondwana dispersion and Asian accretion: Tectonic and paleogeographic evolution of eastern Tethys; *J. Asian Earth Sci.* **66** 1–33.

Patel R C, Singh P and Lal N 2015 Thrusting and back-thrusting as post-emplacement kinematics of the Almora klippe: Insights from low-temperature thermochronology; *Tectonophys.* **653** 41–51, https://doi.org/10.1016/j.tecto.2015.03.025.

Song Y, Su L, Dong J, Song S, Allen M B, Wang C and Hu X 2020 Detrital zircons from Late Paleozoic to Triassic sedimentary rocks of the Gongshan–Baoshan Block, SE Tibet: Implications for episodic crustal growth of Eastern Gondwana; *J. Asian Earth Sci.* **188** 104106.

Trivedi J R, Gopalan K and Valdiya K S 1984 Rb-Sr ages of granitic rocks within the Lesser Himalayan nappes, Kumaun, India; *Geol. Soc. India* **25** 641–654.

Valdiya K S 1980 *Geology of Kumaun Lesser Himalaya*; Wadia Institute of Himalayan Geology Publication, Dehradun.

Vermeesch P 2018 IsoplotR: A free and open toolbox for geochronology; *Geosci. Front.* **9**(**5**) 1479–1493.

Corresponding editor: Rajneesh Bhutani